Synthesis, Characterization, and Electrocatalytic Activity of PtBi Nanoparticles Prepared by the Polyol Process

Chandrani Roychowdhury, Futoshi Matsumoto, Paul F. Mutolo, Héctor D. Abruña, and Francis J. DiSalvo*

Department of Chemistry and Chemical Biology, Baker Laboratory, Cornell University, Ithaca, New York 14853-1301

Received August 22, 2005. Revised Manuscript Received September 21, 2005

Polycrystalline networks of nanoparticles of the ordered intermetallic phase of PtBi have been prepared at 160 °C using the polyol process. In this reaction the polyol acts as both the solvent and the reducing agent. Powder X-ray diffraction (pXRD) studies confirm the presence of the ordered intermetallic phase with an average grain size of ∼19 nm. Electron microscopy studies show that these grains are agglomerated in open networks. pXRD and scanning electron microscopy (SEM) show that the reaction proceeds through an intermediate phase and that the morphology of the particles changes during the course of the reaction. The products have been characterized by SEM, STEM, EDX, CBED, and EELS. The surface area of the nanoparticles has also been measured via BET using krypton as the adsorbing gas. The electrocatalytic activity of the PtBi intermetallic phase towards the oxidation of formic acid has been studied by cyclic voltammetry. The as-prepared PtBi nanoparticles exhibited enhanced electrocatalytic activity when compared to that of Pt nanoparticles and PtRu nanoparticles in terms of both oxidation onset potential and current density.

Introduction

Nanophase powders of elemental metals and some of their alloys are currently used in a variety of technical fields because they possess specific and remarkable properties. Due to their high proportion of surface vs bulk atoms, the surface area, the reactivity of these materials is significantly higher than that of coarse particles, making them ideal candidates for powder metallurgy or catalytic applications. Metal nanoparticles for catalytic applications have been prepared by various techniques but most often by chemical reduction and precipitation from aqueous or organic solutions.[1−6] Chemical reduction of metal species in ethylene glycol under different reaction conditions is the basis of the so-called polyol process.[7] This technique has been used since the 1980s to prepare small particles (some as small as a few nanometers) of many metals, such as Ni, Bi, Co, Ag, Au, Pd, and Pt.[7−12] An advantage of this method of metal particle synthesis is that metal particle formation takes place in solution and at temperatures well below those used in standard solid-state methods. Synthesis of metal particles using the polyol process requires dissolution of the metal precursor in a liquid polyol (often ethylene glycol but also triethylene glycol or tetraethylene glycol).[13,14] The reaction rate is controlled by adjusting the temperature to achieve the controlled reduction of the solvated metal species, condensation of metal atoms from solution, and finally formation of metal particles. The liquid polyol serves as both solvent and reducing agent, and it often acts as a protecting agent, preventing interparticle sintering. A rigorous control of the different reaction parameters such as temperature, precursor type, amount, and order of addition of reactants allows control of the size, shape, and size distribution of the particles. Each metal synthesis is therefore a special case that requires optimization of conditions.

Even though the polyol process has been widely used for the synthesis of nanoparticles of many metals, the mechanisms involved in the different stages of the overall reaction are not fully understood, and control of the process remains largely an empirical task.

Bimetallic alloys (solid solutions) have also been prepared by the polyol process[14−18], though these have not been studied as extensively as elemental particles. Schaak et al. synthesized nanocrystals of AuCu and $AuCu_3$ by a modified polyol process.[14] Chow et al. synthesized nanosized Co−Cu par-

* To whom correspondence should be addressed. E-mail: fjd3@cornell.edu.

(1) Komarneni, S.; Li, D.; Newalkar, B.; Katsuki, H.; Bhalla, A. S. *Langmuir* **2002**, *18*, 5959.
(2) Alivisatos, A. P. *Science* **1996**, *271*, 933.
(3) Ahmadi, T. S.; Wang, Z. L.; Green, T. C.; Henglein, A.; El-Sayed, M. A. *Science* **1996**, *272*, 1924.
(4) Pileni, M. P. *Langmuir* **2001**, *17*, 7476.
(5) Teranishi, T.; Hosoe, M.; Tanaka, T.; Miyake, M. *J. Phys. Chem. B* **1999**, *103*, 1805.
(6) Cushing, B. L.; Kolesnichenko, V. L.; O'Connor, C. J. *Chem. Rev.* **2004**, *104*, 3893.
(7) Figlarz, M.; Fievet, F.; Lagier, J.-P. French Patent No. 8221483, 1985.
(8) Figlarz, M.; Ducamp-Sanguesa, C.; Fievet, F.; Lagier, J.-P. *Powder production and spray forming-advances in powder metallurgy and particulate materials*; 1992; Vol. 1.
(9) Ducamp-Sanguesa, C.; Herrera Urbina, R.; Figlarz, M. *J. Solid State Chem.* **1992**, *100*, 272.
(10) Silvert, P.-Y.; Tekaia-Elhsissen, K. *Solid State Ionics* **1995**, *82*, 56.
(11) Bonet, F.; Grugeon, S.; Dupont, L.; Herrera Urbina, R.; Tekaia-Elhsissen, K.; Tarascon, J. M. *Solid State Sci.* **2002**, *4*, 665.
(12) Chen, J.; Herricks, T.; Geissler, M.; Xia, Y. *J. Am. Chem. Soc.* **2004**, *126*, 10854.
(13) Grisaru, H.; Palchik, O.; Gedanken, A.; Palchik, V.; Slifkin, M. A.; Weiss, A. M. *Inorg. Chem.* **2003**, *42*, 7148.
(14) Sra, A. K.; Ewers, T. D.; Schaak, R. E. *Chem. Mater.* **2005,** *17* (4), 758.

10.1021/cm051886e CCC: $30.25
Published on Web 10/26/2005

ticles by this technique.[16] Co−Ni and Fe−Ni particles have also been prepared by Viau et al.[17] The same technique was used by Lu et al.[18] to synthesize a PVP-protected Cu−Pd alloy with a high copper content. However, to the best of our knowledge, no intermetallic compounds with an ordered crystalline structure have been directly prepared by the polyol process.

In the last few decades there has been mounting interest in the direct conversion of chemical energy to electricity via fuel cells. In transportation the use of fuel cells would circumvent Carnot cycle limitations and can, in principle, supply energy with efficiencies in excess of 80% depending on the fuel used.[19] Hydrogen is often seen as a likely fuel for fuel cells since mechanistically it is easiest to oxidize. However, H_2/O_2 fuel cells require either on-site H_2 storage or an onboard reformer to extract H_2 from organic fuels. As an alternative, and for smaller, portable applications, there has been a growing drive to study the direct electrocatalytic oxidation of small organic molecules (SOMs) for potential use as fuels in so-called direct fuel cells.[20]

Oxidation of any fuel requires use of a catalyst to achieve the current densities needed for practical applications, and platinum-based alloys, especially PtRu, are among some of the most efficient catalysts for oxidation of SOMs.[21] As mentioned elsewhere,[22] oxidation of formic acid is useful as a model system for studying electrochemical oxidation of simple alcohols (e.g., methanol, ethanol). Mechanistically, oxidation of these molecules involves an adsorbed carbon monoxide intermediate ($-CO_{ads}$). Pure platinum electrodes are readily poisoned by these intermediates, greatly reducing their utility in commercial direct alcohol (e.g., DMFC) or formic acid fuel cells. The utility of PtRu alloys over Pt stems from the diminution of the overpotential required to oxidize these intermediates from the PtRu surface.

We recently reported[22,23] a new approach in the search for electrocatalysts to replace PtRu with less expensive materials and to avoid inherent problems of using disordered alloys as catalysts such as segregation and poisoning by CO and sulfur-containing materials. In place of the disordered PtRu alloy, the ordered intermetallic phase, PtBi, was studied as an electrocatalyst for formic acid oxidation. As a bulk material, PtBi exhibited high electrocatalytic activity toward formic acid oxidation and great tolerance toward poisoning by CO. However, to incorporate these materials into actual fuel cells they need to be prepared in nanoparticle form, so as to have increased surface area, which, in turn, should lead to enhanced electrochemical activity per platinum atom.

In this paper we present the synthesis via the polyol process of the stoichiometric intermetallic compound PtBi. Reactants include chlorides and nitrates of platinum and bismuth and ethylene glycol as the solvent and reducing agent. The influence of the experimental conditions on the final products is discussed. Characterization of the products has been performed using powder X-ray diffraction (pXRD), scanning electron microscopy (SEM), scanning transmission electron microscopy (STEM), convergent beam electron dispersion (CBED), electron energy loss spectroscopy (EELS), and energy-dispersive X-ray microanalysis (EDX). The electrocatalytic activity of the PtBi intermetallic phase toward the oxidation of formic acid has been studied by cyclic voltammetry. The as-prepared PtBi nanoparticles exhibited enhanced electrocatalytic activity when compared to that of Pt black and PtRu nanoparticles in terms of both oxidation onset potential and current density.

Experimental Section

Materials. With the exception of H_2PtCl_6, all chemicals used were reagent grade. Bismuth nitrate ($Bi(NO_3)_3 \cdot 5H_2O$ (Allied Chemical)) and hexachloroplatinic(IV) acid (H_2PtCl_6) were used as metal precursors. $H_2PtCl_6 \cdot xH_2O$ was prepared by oxidizing Pt metal with aqua regia.[24] Ethylene glycol (Mallinckrodt) was used as the solvent and reducing agent. Distilled water and acetone (Aldrich) were used to wash the products. The water was purified with a Millipore Milli Q system.

Synthesis of Nanoparticles. A 60 mL amount of ethylene glycol was degassed with argon for 2 h. Between 0.2 and 0.3 g of $Bi(NO_3)_3 \cdot 5H_2O$ was dissolved in this ethylene glycol in a three-neck round-bottomed flask under magnetic stirring. The flask was continuously purged with argon. A condenser was attached to the flask, and the solution was heated to 160 °C in an oil bath and maintained at this temperature for 16 h. The solution color changed from colorless to white and finally to dark gray. In a separate round-bottomed flask, 60 mL of ethylene glycol was purged with argon. A stoichiometric amount, relative to the Bi precursor, of $H_2PtCl_6 \cdot xH_2O$ was dissolved in this ethylene glycol to yield an orange solution. This orange solution was transferred to an addition funnel and after dropping the temperature to 145 °C was added to the hot, gray Bi-containing solution over 3 h. The solution turned black within 5 min of beginning the addition of H_2PtCl_6, and eventually a black product separated out. In three separate experiments, the mixtures, after addition of H_2PtCl_6, were heated at 145 °C for an additional (A) 6, (B) 24, and (C) 48 h. At the end of the total reaction time of 25 (16 + 3 + 6), 43 (16 + 3 + 24), or 67 h (16 + 3 + 48), the mixture was cooled to room temperature by taking it out of the oil bath. The solid powder was separated from the supernatant by centrifugation and subsequently washed three times each with distilled water and acetone in order to remove the organic phase. After each washing step the solids were also separated from the liquid by centrifugation. Afterward, the powders were dried under vacuum at room temperature.

Characterization. An X-ray powder diffraction powder pattern (Scintag XDS 2000) was taken of the black PtBi nanoparticles to confirm the composition and structure of the intermetallic phase.

(15) Bonet, F.; Grugeon, S.; Dupont, L.; Herrera Urbina, R.; Guery, C.; Tarascon, J. M. *J. Solid State Chem.* **2003**, *172*, 111.
(16) Chow, G. M.; Kurihara, L. K.; Kemmer, K. M.; Schoen, P. E.; Elam W. T.; Ervin, A.; Keller, S.; Zhang, Y. D.; Budnick, J.; Ambrose, T. *J. Mater. Res.* **1995**, *10*, 6.
(17) Viau, G.; Fiévet-Vincent, F.; Fiévet, F. *Solid State Ionics* **1996**, *8*, 259.
(18) Lu, P.; Dong, J.; Toshima, N. *Langmuir* **1999**, *15*, 7980.
(19) Lamy, C. L.; J.-M.; Srinivasan, S. *Direct Methanol Fuel Cells: From a Twentieth Century Electrochemist's Dream to a Twenty-first Century Emerging Technology;* Kluwer Academic/Plenum Publishers: New York, 2001; Vol. 34.
(20) Parsons, R.; VanderNoot, T. *J. Electroanal. Chem.* **1988**, *257*, 9.
(21) Schmidt, T. J.; Gasteiger, H. A.; Behm, R. J. *J. Electrochem. Soc.* **1999**, *146*, 1296.
(22) Casado-Rivera, E.; Volpe, D. J.; Alden, L.; Lind, C.; Downie, C.; Vázquez-Alvarez, T.; Angelo, A. C. D.; DiSalvo, F. J.; Abruña, H. D. *J. Am. Chem. Soc.* **2004**, *126*, 4043.
(23) Casado Rivera, E.; Gál, Z.; Angelo, A. C. D.; Lind, C.; DiSalvo, F. J.; Abruña, H. D. *Chem. Phys. Chem.* **2003**, *4*, 193.
(24) *Inorganic Syntheses*; Holtzclaw, H. F., Jr., Ed.; McGraw-Hill: New York, 1966; Vol. VIII, 239.

The particle morphology and size were studied by scanning electron microscopy (SEM) using a LEO-1550 field emission SEM (FE-SEM). Scanning TEM images, energy-dispersive analysis by X-rays (EDX), electron energy loss spectroscopy data (EELS), and convergent beam electron diffraction (CBED) data were collected on a VG HB501UX UHV STEM. To measure the surface area of the samples a Micromeritics ASAP 2020 was used to collect a partial adsorption isotherm at liquid nitrogen temperature (−196 °C) with krypton as the adsorption gas over the pressure range (P/P_0) of 0.06 and 0.5. Prior to measurements the sample was degassed at room temperature for 48 h. The specific surface area was determined according to the Brunauer−Emmett−Teller (BET) method in the relative pressure (P/P_0) range of 0.08−0.185.

Electrocatalytic Activity. The electrocatalytic activity of the PtBi nanoparticles was tested using formic acid as the fuel. Prior to each experiment a suspension of the nanoparticle catalyst was prepared. To prepare the suspension, 4 mg of the dried PtBi nanoparticle sample was weighed out. To this, 3.98 mL of distilled water and 1 mL of isopropyl alcohol (Aldrich) were added. 20 μL of 5% w/w Nafion solution in alcohols and water (Aldrich, EW: 1100) were added to this mixture. The resulting mixture was sonicated in a bath-type ultrasonicator for 4 h. Suspensions of Pt nanoparticles (Alfa Aesar, HiSPEC TM 1000, ADS: 2−3 nm, surface area 27 m^2/g) and 50:50 PtRu alloy nanoparticles on Vulcan XC-72R (E-TEK, surface area 107 m^2/g [25]) were prepared using the same method.

The nanoparticle suspension described above was coated onto a 3 mm diameter glassy carbon disk (GC) electrode. The electrode had been previously polished with diamond paste (METADI-Buehler, ø = 1 μm) and ultrasonicated in Millipore water (18 MΩ cm^{-1}, Millipore Milli-Q) for 10 min. The electrode was then rinsed with Millipore water and allowed to dry in air. A 70 $\mu g\ cm^{-2}$ amount of the nanoparticles (6.1 μL of the nanoparticle suspension) was coated onto the clean glassy carbon electrode. The electrode was then spin dried at 600 rpm under a nitrogen gas atmosphere.

Formic acid oxidation on the nanoparticle-coated glassy carbon electrode was examined in a mixture of 0.125 M formic acid (Mallinckrodt, 88% analytical reagent)/0.1 M sulfuric acid (J. T. Baker ultrapure reagent) at a sweep rate of 10 mV s^{-1}. All solutions were prepared with Millipore water and deaerated with prepurified nitrogen for at least 10 min. The measurements were conducted at room temperature. All potentials are referenced to a sodium chloride saturated Ag/AgCl electrode without regard for the liquid junction.

Results and Discussion

Since the standard reduction potentials of pure Bi and Pt are +0.31 and +1.3 V, respectively,[26] Pt is more easily and rapidly reduced than Bi. Thus, when platinum and bismuth precursors are added together to ethylene glycol and heated, the major product is metallic platinum. Consequently, we added the more slowly reducing bismuth precursor to the solution first and allowed the partial reduction of $Bi(NO_3)_3$ to proceed before adding the platinum salt. It should be noted that the bismuth precursor could be completely reduced to bismuth without addition of platinum, but the reaction was much slower owing to the relative difficulty of reducing bismuth. The final product (pure Bi nanoparticles, ∼80 nm domain size) in that case was formed after prolonged heating

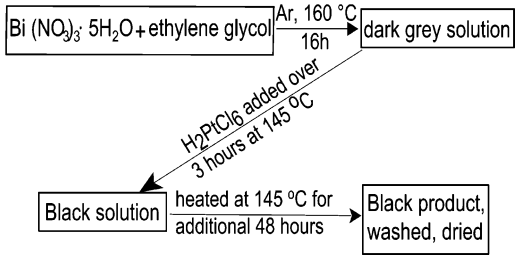

Figure 1. Schematic illustration detailing all major steps and changes involved in the formation of ordered PtBi nanoparticles from starting precursors.

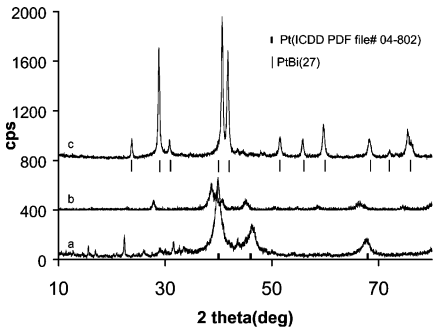

Figure 2. pXRD patterns of PtBi samples that were prepared by varying the final refluxing time, keeping the temperature at 145 °C. The bottom pattern (a) is for the reaction where the refluxing time was 6 h (total reaction time of 25 h). The middle pattern (b) is that for 24 h refluxing time (total reaction time of 43 h), while the top pattern (c) is at the end of the reaction for 48 h refluxing time (total reaction time of 67 h). Markers for pattern c signify PtBi[27], while markers for pattern a signify Pt.

(120 h) at 160 °C. On the other hand, when the platinum precursor was added reduction of bismuth was accentuated and the final product PtBi was formed after only 48 h of heating. This led us to conclude that the Pt nanoparticles that are formed on adding the Pt precursors to the partially reduced Bi solution catalyze the further reduction of the bismuth precursor. We adjusted temperature and times of reduction and addition to optimize the purity of the PtBi product. Figure 1 summarizes all the major steps and changes involved in a typical synthesis. It is important to note that the H_2PtCl_6 solution in ethylene glycol must be added slowly over 3−4 h to the partially reduced Bi solution. In the experiments where the Pt solution was added quickly over 5−10 min the pXRD pattern of the resulting product showed that elemental Pt was the major phase and PtBi was a minor phase. Prolonged heating in ethylene glycol did not lead to the formation of additional PtBi in this case. Figure 2 shows the pXRD patterns of the PtBi samples prepared by varying the final heating time while keeping the refluxing temperature constant at 145 °C. It can be seen from Figure 2 that for refluxing times of 6 (total reaction time 25 h, pattern a) and 24 h (total reaction time 43 h, pattern b) the pXRD indicates the presence of both Pt (ICDD PDF file # 04−802) and PtBi.[27] On the other hand, the pXRD of the product from the reaction with 48 h refluxing time (total reaction time 67 h, pattern c) shows the presence of only single-phase PtBi.[27] This led us to conclude that the final refluxing time has an important effect on the composition of the product and that a full 48 h of refluxing after H_2PtCl_6 addition is needed for

(25) Chai, G. S.; Yoon, S. B.; Choi, J. H.; Sung, Y. E. *J. Phys. Chem. B* **2004**, *108*, 7074.
(26) Lide, D. R. *CRC handbook of Chemistry and Physics*, 73rd ed.; CRC Press, Boca Raton, FL, 1992; Vols. 8−18, p 20.
(27) Zhuravlev, N. N.; Stepanova, A. A. *Sov. Phys.-Crystallogr.* **1962**, *7*, 241.

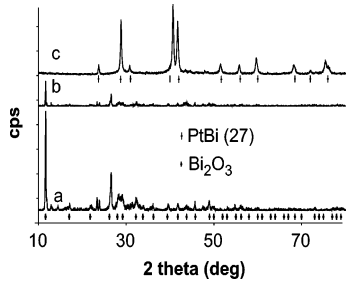

Figure 3. pXRD pattern of reaction mixture solids that were withdrawn from the reaction flask after (a) 9, (b) 16, and (c) 67 h heating (at the end of the reaction time). Patterns a and b index for Bi_2O_3 (ICDD file# 71-0467), Bi (ICDD PDF file # 44-1246), and $Bi(NO_3)_3$ (ICDD PDF file# 44-314), while pattern c indexes only for PtBi[27]. The average domain size of the final product calculated from pattern c by the Scherrer equation is 19 nm. Markers for pattern c signify PtBi[26], and markers for pattern a signify Bi_2O_3.

the complete transformation of elemental Pt and Bi to the intermetallic PtBi phase. The domain size of the product was calculated from the Scherrer formula: −size (nm) = 0.94 × 0.154/fwhm (radians) × cos θ (radians). The average domain size was approximately 19 nm for all the samples.

To obtain a clearer understanding of the reaction mechanism the reaction products were monitored over time by pXRD and SEM. Aliquots of the product were withdrawn from the reaction flask after (a) 9, (b) 16, and (c) 67 h (at the end of the reaction) into test tubes filled with argon. The aliquots were washed with degassed water and acetone and vacuum-dried to collect the solid. Figure 3 shows the pXRD of these solids that were collected after (a) 9 (bottom), (b) 16 (middle), and (c) 67 h (top). The peaks in the 9 and 16 h patterns index chiefly for Bi (ICDD PDF file # 44−1246), Bi_2O_3 (ICDD PDF file# 71−0467), and unreduced $Bi(NO_3)\cdot 5H_2O$ (ICDD PDF file# 44−314). Some of the peaks in the pXRD pattern could not be indexed. These could be peaks from a complex that is being formed between the bismuth and the polyol. No peaks from platinum or platinum compounds were expected or observed since the platinum precursor is not added until just after 16 h. pXRD of the final product (c) indicated the presence of single-phase PtBi[27] ($P6_3/mmc$, a = 4.315 Å, c = 5.490 Å).

SEM images were taken of the solids obtained at different stages of the reaction. Figure 4 shows the SEM images that were taken by withdrawing aliquots of the product from the reaction flask after (a) 9, (b and c) 16, and (d) 67 h. It can be seen from the figures that the morphology of the product changes during the course of the reaction. In the earlier stages of the reaction, when the $Bi(NO_3)_3\cdot 5H_2O$ is being reduced by ethylene glycol to elemental Bi, long platelike structures 2−6 μm in length and 160−200 nm in width (Figure 4a) are apparent. Further heating caused these plates to become porous and almost spongelike in appearance (Figure 4b), with tetrapodic growth on the surfaces (Figure 4c). The SEM image of the final product (Figure 4d) shows regular spherically shaped particles with diameters from 35 to 60 nm. The product appears to be highly aggregated, and thus the domain size as calculated from the Scherrer equation is smaller than the particle size.

We investigated the possibility of making smaller nanoparticles by adding surfactants such as poly(vinylpyrrolidone)

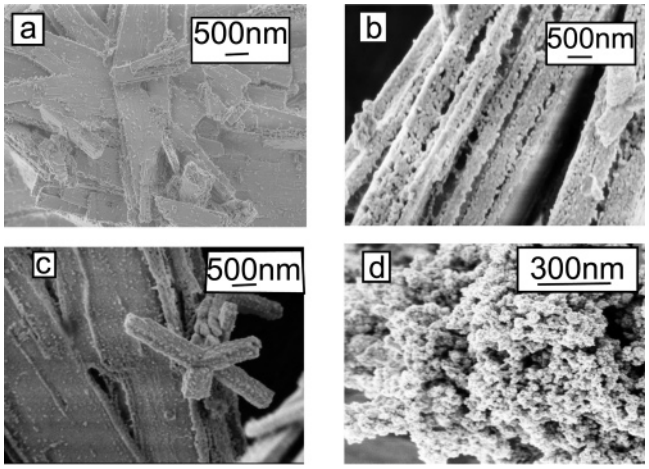

Figure 4. SEM images of reaction solids that were withdrawn from the reaction flask at different time intervals: (a) 9, (b and c) 16, and (d) 67 h. Images a, b, and c show the morphology of the Bi intermediate formed before Pt addition. Image d shows the morphology of the final product.

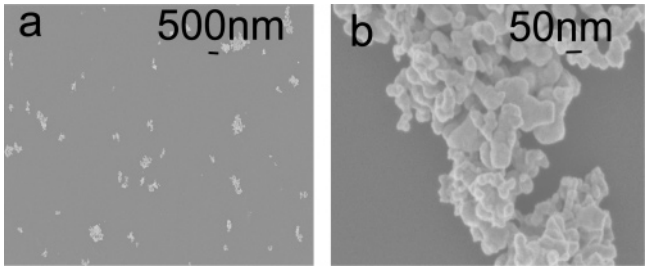

Figure 5. SEM images of PtBi nanoparticles suspended in ethanol by ultrasonication. The aggregated networks as well as unaggregated particles can be seen.

(PVP) to the reaction mixture. However, we found it difficult to remove the PVP from the surface of the nanoparticles by any chemical means (washing, etc.), and heat treatment to burn off the organic surfactants would result in sintering of the nanoparticles, causing larger particles to be formed and thus diminishing the surface area further. Also, since these materials have potential use as fuel cell electrocatalysts, adding surfactants could result in blockage of the nanoparticle surfaces and thus cause a diminution in catalytic activity. This, is turn, would render the materials much less attractive for use in fuel cells as catalysts.

We also investigated the possibility of using different bismuth precursors, notably $BiCl_3$. However, owing to the very limited solubility of most bismuth precursors in ethylene glycol, the stoichiometry of the reactions could not be controlled, and hence, we did not pursue using other precursors.

Further SEM images were obtained by dispersing the final product in various solvents and drying the suspensions on silicon (100) wafers. The solvents used were methanol, ethanol, 2-propanol, acetone, tetrahydrofuran, dichloromethane, and diethyl ether. To make the suspensions about 2 mg of the final product was weighed into a clean test tube to which 10 mL of the solvent was added. The solution was then sonicated using an immersion-type ultrasonicator for 20 min to form gray−black dispersions of the nanoparticles. Two drops of each of the dispersions were coated on a clean silicon (100) wafer and then air-dried. Figure 5a and b shows the SEM images of PtBi nanoparticles suspended in ethanol

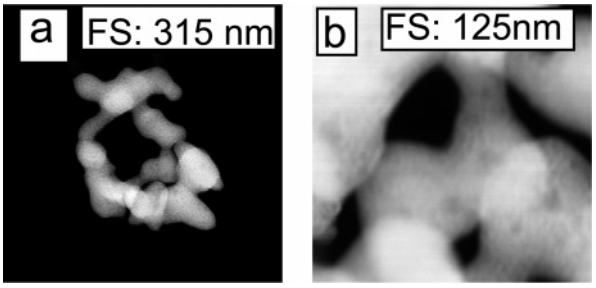

Figure 6. STEM images showing PtBi nanocrystalline networks at different magnifications (note: FS indicates full scale).

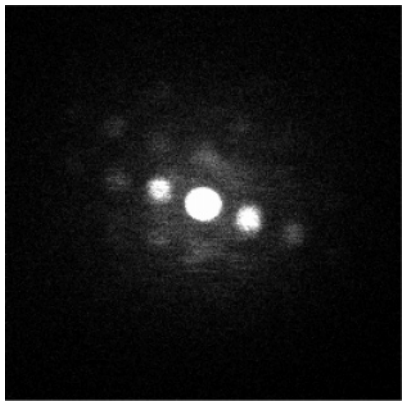

Figure 7. Convergent beam electron diffraction pattern (CBED) of 20−30 nm PtBi nanocrystalline networks

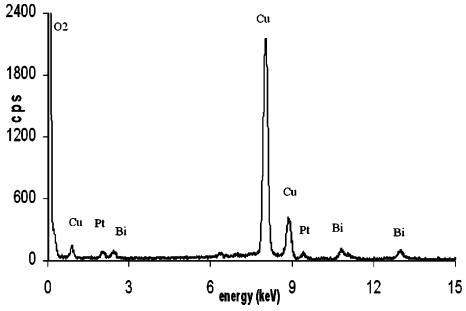

Figure 8. EDX spectrum showing the presence of Pt and Bi in the PtBi sample. The copper and oxygen peaks correspond to the copper oxide from the holder.

and coated on a Si (100) wafer. It is clear from the images that ultrasonication separates the agglomerated particles to some extent into smaller clumps and individual grains.

STEM analysis was performed on PtBi samples that had been prepared after a total reaction time of 67 h. Figure 6 shows the STEM images that were recorded at different resolutions. Figure 6a and b show that the particles were highly aggregated, forming open networks or chains as clearly evident in the SEM images. The images have a somewhat cloudy appearance, due to possible charging of the bismuth oxides that could likely be coating the surface (Figures 4d, 5a, and 5b).

The smallest PtBi particles are single-crystal domains, as shown by the CBED pattern (Figure 7). The semiquantitative EDX spectrum taken in the STEM (Figure 8) shows the presence of Pt and Bi (49 ± 2 atom % Pt, 51 ± 2 atom % Bi), thus corroborating that the product consisted of Pt and Bi. The EELS spectrum, however, shows evidence of oxygen being present in the sample (Figure 9). This leads us to believe that there may be an amorphous oxygen-containing

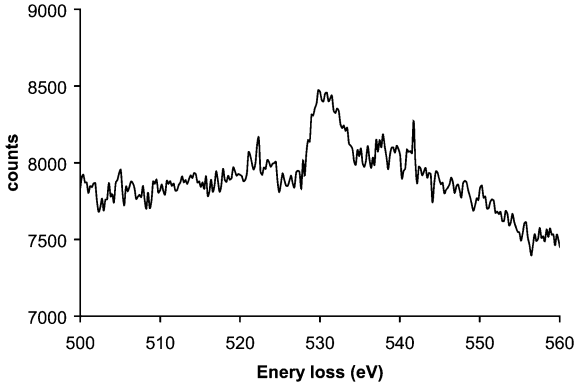

Figure 9. EELS spectrum showing the presence of oxygen (peak at 532 eV) in the PtBi sample.

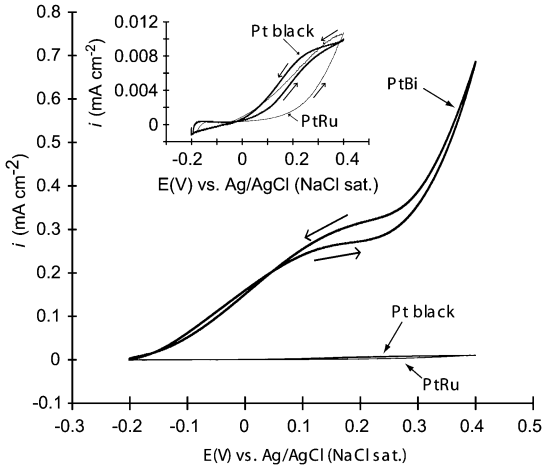

Figure 10. Cyclic voltammograms (CVs) for formic acid oxidation on 4 nm Pt black, 19 nm PtBi nanoparticles, and 1:1 PtRu alloy nanoparticles on Vulcan XC72R, as labeled. (Inset) CV scaled to reveal Pt and PtRu activity (note reduced *y*-axis scale). All data measured for 0.125 M formic acid in 0.1 M sulfuric acid (scan rate 10 mV s^{-1}).

layer (possibly organic) coating the sample, which also leads to some blurring of the CBED pattern.

The surface area of the PtBi sample (19 nm domain size) was measured by collecting a partial adsorption isotherm at liquid nitrogen temperature and using krypton as the adsorbing gas. The specific surface area was determined according to the Brunauer−Emmett−Teller (BET) method in the relative pressure (P/P_0) range of 0.08−0.185 and was found to be 2.1 m^2/g. The *c* value (reflects the strength of interaction between the krypton and the surface) was 10.5, and the correlation coefficient of the BET fit was 0.999987. From the BET surface area the particle size was calculated to be approximately 184 nm, which is consistent with the size of the *aggregated* networks of the nanoparticles but not the individual domains.

Figure 10 shows the cyclic voltammograms for formic acid oxidation on the three different nanoparticle catalyst electrodes; Pt, PtRu, and PtBi. Two parameters of particular importance in comparing the relative activity of these electrocatalysts are onset potential (reflecting thermodynamic aspects) for oxidation and current density (reflecting kinetics). Clearly, the more negative the onset potential and the higher the current density, the better the catalyst.

In terms of onset potentials, the Pt, PtRu, and PtBi nanoparticle electrodes exhibited onset potentials of +100,

Table 1. Onset Potentials and Current Density at Different Voltages for Pt Black, PtRu, and PtBi Nanoparticles for Formic Acid Oxidation

		current density (mA cm^{-2})			
catalyst	onset potential (mV)	−100 mV	0 mV	+100 mV	+200 mV
Pt black	+100	−0.0015	0.0008	0.0034	0.007
PtRu	+150	−0.0015	0.001	0.003	0.0054
PtBi	−160	0.05	0.16	0.26	0.33

+160, and −160 mV, respectively (see also Table 1). An analysis of these numbers immediately makes manifest that PtBi has superior electrocatalytic activity when compared to both Pt and PtRu. In addition, the value for PtBi nanoparticles is also in accord with values obtained for bulk PtBi samples.[22] This is an important observation since it indicates that the electrocatalytic properties of the bulk materials are retained at the nanoscale.

The current density at a specified potential is a clear measure of electrocatalytic efficacy. However, in making comparisons one needs to take into account the fact that the different samples had different particle size (and distribution). Thus, to make meaningful comparisons the currents were normalized to the measured surface area of the respective catalysts (see Experimental Section for details). Values of the current density for the different materials at various potentials are presented in Table 1. The magnitude of the current density, especially at lower potentials (which is the region of most interest to fuel cell applications), shows that the PtBi electrode has far superior activity when compared to Pt and PtRu. For example, at 0.0 V (vs Ag/AgCl) PtBi nanoparticles exhibited a current density that was 160 times that of PtRu and 200 times that of Pt.

It is also of note to look at the shape of the voltammetric profile. From Figure 10 it is clear that both Pt and PtRu (and especially PtRu) exhibit a great deal of hysteresis. On the other hand, while PtBi exhibits some hysteresis at high potentials, it is virtually nonexistent at potentials up to +100 mV. Such behavior can be attributed, at least in part, to poisoning effects by CO. Whereas both Pt and PtRu can be poisoned by CO, PtBi exhibits a great deal of tolerance to CO poisoning, which is reflected in the virtual absence of hysteresis in the voltammetric profile. (It should also be mentioned that the hysteretic response can also arise from surface oxide formation at very positive applied potentials.)

From the above discussion it is evident that PtBi nanoparticles are vastly superior in performance to both Pt and PtRu nanoparticles in terms of both the onset potential as well as current density. Thermodynamically (as evidenced by the onset potential) PtBi exhibits a greatly diminished overpotential for oxidation compared to Pt ($\Delta E = 260$ mV) and PtRu ($\Delta E = 310$ mV). Similarly, the current densities, especially at low potentials, are dramatically higher for PtBi when compared to both Pt and PtRu (see Table 1).

It is also important to note that these are our first attempts at synthesizing nanoparticles of ordered intermetallic phases such as PtBi. As a result, we have not optimized any of the operational parameters of the synthesis. This is to be contrasted with Pt black and especially PtRu nanoparticles (from E-TEK), which have been optimized for fuel cell applications. Yet even under these nonoptimized conditions PtBi clearly exhibits superior activity to both Pt and PtRu. Thus, at this time the activity enhancements, which are very large, can still be considered lower limits.

Conclusions

In this paper we have demonstrated a new low-temperature approach to the synthesis of polycrystalline networks of nanoparticles of the ordered intermetallic phase of PtBi using the polyol process. In this reaction the polyol acted as both the solvent and the reducing agent. Powder X-ray diffraction (pXRD) studies confirmed the presence of the ordered intermetallic phase with average grain size of ∼19 nm. It was shown by electron microscopy studies that these grains are agglomerated in open networks. The BET surface area of the nanoparticles was found to be 2.1 m^2/g, and this was consistent with the size of the aggregated networks. pXRD and scanning electron microscopy (SEM) also showed that the reaction proceeded through an intermediate phase of bismuth and that the morphology of the particles changed during the course of the reaction. Formation of the final product must take place through the reaction of platinum nanoparticles with larger bismuth particles. This reaction must occur through solid-state diffusion but over small length scales of approximately 20 nm. Since this process involves production of an intermediate phase, it does not appear that the particle (domain) sizes could be easily controlled by adding surfactants or changing the process conditions. The as-prepared PtBi nanoparticles exhibit enhanced electrocatalytic activity toward formic acid oxidation when compared to Pt black and PtRu nanoparticles in terms of both onset potential and current density.

Acknowledgment. The authors thank Malcolm Thomas at the Cornell Center for Materials Research for help with the STEM data collection. This work was supported by DOE Grant DE-FG02-03ER46072. The STEM, microprobe, and SEM data were obtained in the shared experimental facilities managed by the Cornell Center for Materials Research, a MRSEC center supported under NSF grant DMR-0079992. C.R.C. would like to thank Scott Warren at the Materials Science and Engineering Department at Cornell University for helping with the BET surface area measurements.

CM051886E